Robust Ion-Implantation Process Design Through Statistical Analysis

C. Sudhama, Rainer Thoma, Mike F. Morris, Jim Christiansen and Ik-Sung Lim

Motorola Digital DNA Laboratories

Maildrop EL615, 2100 E. Elliot Road, Tempe, AZ 85284, USA, c.sudhama@motorola.com

ABSTRACT

This paper demonstrates the importance of taking statistical process variations into account when designing semiconductor processes, and provides a methodology for doing so. An on-axis, high-energy ion-implant process is used as a vehicle to demonstrate the methodology. UT-MARLOWE is the well-calibrated (and hence predictive) simulation tool of choice. It is shown that crystal-cut errors and implanter-tilt errors can result in a considerably off-axis implant for this nominally on-axis implant: instead of the intended *tilt = 0°*, the implant actually occurs at an average tilt of ~*0.65°*, with a significant probability of having *tilt > 1°*. Knowledge of the error-statistics is used to design a robust process (i.e. a process relatively immune to statistical process variations), thereby providing better control over device performance. This methodology can also account for deterministic errors arising from beam divergence and process-disk geometry in multi-wafer machines.

Keywords: Statistical-process-error, ion-implantation, tilt, angle, process-design

1 INTRODUCTION

Predictive simulation of processes such as ion-implantation is important in technology development [1-2]. UT-MARLOWE, a state-of-the-art Monte-Carlo simulator [3], is found to be very accurate in Motorola for simulating implant profiles at various energies, and is thus considered to be predictive, especially for high-energy profiles in the sub-1MeV range.

An on-axis *(tilt=0°)*, *750keV*, *phosphorus* implant through a ~*60Å* screen oxide is used as a case-study. As shown in Fig. 1, UT-MARLOWE predicts a second (deeper) peak which is not seen in the SIMS data; this spurious doping peak can strongly affect simulated electrical characteristics of certain devices. Such errors in predicted profiles must therefore be avoided. We find that the discrepancy actually arises from random fabrication process errors neglected till now. These errors are described in the next section.
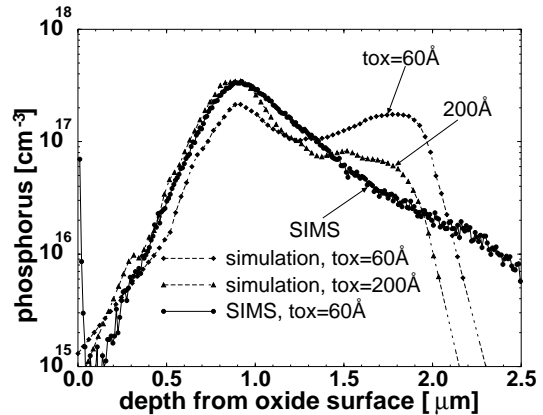

Figure 1. Measured (SIMS) and simulated profiles for an on-axis, *750keV*, *2e13cm⁻²* phosphorus implant through *60Å* of oxide. The discrepancy is due to random errors in tilt.

In this work, for the first time, we present a TCAD methodology to rigorously account for statistical variations due to these random process errors (inherent in all semiconductor processes), and thereby design a robust ion-implantation process.
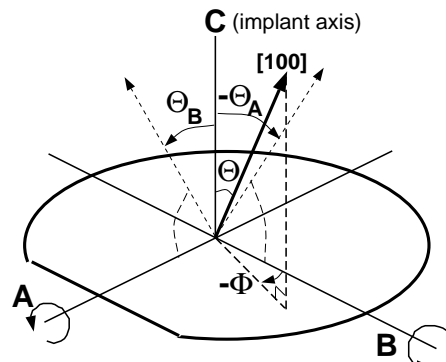
2 RANDOM PROCESS ERRORS

Figure 2. Cartesian co-ordinates *(axes A, B, C)* used to quantify tilt-errors & the polar system *(r, Θ, Φ)* used to specify implants. Both are referenced to the wafer flat and wafer perpendicular.

One source of random error in the ion-implantation process is crystal-cut misalignment, which occurs in the wafer manufacturing process. This causes the *[100]* axis to not coincide with the perpendicular to the wafer surface.

Crystal-cut error is measured using x-ray diffractometry, and is quantified as two tilt-angles about orthogonal axes A and B [4], as illustrated in Fig. 2. This error can thus be represented by random variables (RVs) CUT_A and CUT_B. Statistics for the two RVs are summarized in Table 1 [4]. Evidently, the statistical distribution is very tight, i.e. σ-values are very small.

Table 1. Crystal-cut error statistics from two lots of seventy-five *(100)*-oriented wafers [4]. XRD is used to determine the rotation of the *[100]* vector about axes A and B of Fig. 2.

Crystal-Cut (Slice Alignment) error about axes A and B				
Lot	mean [CUT_A]	mean [CUT_B]	σ [CUT_A]	σ [CUT_B]
1	-0.017°	+0.133°	< 0.017°	< 0.017°
2	+0.033°	-0.167°	< 0.017°	< 0.017°

In addition, misalignments in the implanter can lead to random errors in the tilt angle. These misalignments are measured about the same axes A and B. For low tilt angles, the expected *best-case* accuracy is $\pm 0.5°$ about *each* axis. This implies two RVs, $IMPLANTER_A$ and $IMPLANTER_B$, each with a *mean=0°* and $\sigma=0.5°$. Given only the mean value and standard deviation for an RV, it is necessary to assume a Gaussian probability density for it [5]. Consequently, Gaussian density functions are assumed for the four RVs: $CUT_{A,B}$ and $IMPLANTER_{A,B}$, with the *mean* and σ values mentioned above. For axis A, the total tilt angle (Θ_A) is therefore a RV equal to the sum of CUT_A and $IMPLANTER_A$, and similarly for Θ_B. It is easily shown that the sum of two Gaussian RVs is also a Gaussian RV [6]. Therefore Θ_A and Θ_B are also Gaussian RVs [6], with probability densities described in Eqn. 1 and plotted in Fig. 3.

$$mean_A = mean[\Theta_A] = mean[CUT_A] + mean[IMPLANTER_A], \&$$
$$(\sigma_A)^2 = (\sigma[\Theta_A])^2 = (\sigma[CUT_A])^2 + (\sigma[IMPLANTER_A])^2. \quad (1)$$

Equation 1. Mean and std.-deviation for the total tilt about axis A, which is a Gaussian RV given by $\Theta_A = CUT_A + IMPLANTER_A$. Similarly for Θ_B.
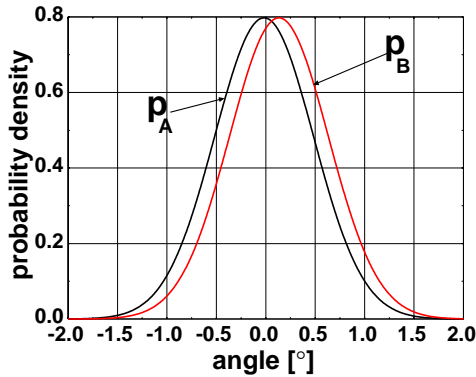

Figure 3. Gaussian probability density functions for the RVs Θ_A and Θ_B as in Equation 1. For this particular case, $\sigma(\Theta_A) = \sigma(\Theta_B) \approx 0.5°$.

It must be noted that tilt and rotation angles commonly used during wafer-processing or implant-simulation, are actually referred to the polar co-ordinate system. It is easily shown using geometrical analysis that for small tilt angles, tilt *(Θ)* and rotation *(Φ)* are given by $(\Theta)^2 = (\Theta_A)^2 + (\Theta_B)^2$, and $\Phi = \Theta_B/\Theta_A$. From these two relationships, the probability density functions for Θ and Φ (both of which are RVs) may easily be derived [6]. The probability density function for Θ is described in Eqn. 2. Here $m^2 = (mean_A)^2 + (mean_B)^2$, $\sigma = \sigma_A = \sigma_B$ and $I_o(x)$ is the modified Bessel function of zeroth order.

$$p_\Theta(\theta) = \frac{\theta}{\sigma^2} I_0\left(\frac{\theta\, m}{\sigma^2}\right) e^{-(\theta^2+m^2)/2\sigma^2}, \, where$$

$$I_0(x) = \frac{1}{2\pi} \int_0^{2\pi} e^{x\cos(t)} dt. \quad (2)$$

Equation 2. Rayleigh-like probability density for random variable Θ, using $(\Theta)^2 = (\Theta_A)^2 + (\Theta_B)^2$. Also see Fig. 4(a).

$$p_\Phi(\phi) = \int_{-\infty}^{+\infty} |\theta_A|\, p_B(\theta_A \phi)\, p_A(\theta_A)\, d\theta_A, \, where$$

$$p_A(\theta_A) = \frac{1}{\sqrt{2\pi}\sigma} e^{-(\theta_A - mean_A)^2/2\sigma^2},$$
$$and\, similarly\, for\, p_B(\theta_B). \quad (3)$$

Equation 3. Cauchy-like probability density, for $\Phi = \Theta_B/\Theta_A$ [6], plotted in Fig. 4(b).

Note that since $m \neq 0$, $p_\Theta(\theta)$ is not a true Rayleigh function; however it does have Rayleigh-like characteristics. Eqn. 3 describes the Cauchy-like probability density function, $p_\Phi(\phi)$, for rotation angle Φ. Note that for this case $mean_A$ and $mean_B$ are non-zero, and therefore analytical solutions for p_Θ and p_Φ are not obtainable. As a result the symbolic equation solver, Mathematica[TM] was used to calculate the functions. These have been plotted in Fig. 4(a) and Fig. 4(b). Incidentally, if $mean_A = mean_B = 0$, $p_\Phi(\phi)$ is a true Cauchy function, given by $p_\Phi(\phi) = 1/(\pi + \pi\, \phi^2)$.
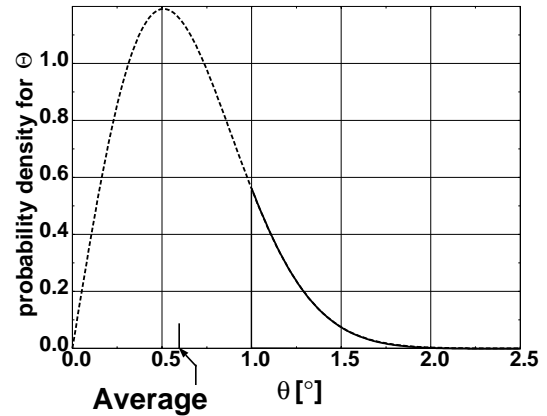

Figure 4(a). Rayleigh-like $p_\Theta(\theta)$ from Eqn. 2. Please see Table 2 for some important properties.

It is evident (see Fig. 4(a)) that for the nominally $0°$ tilt implant, the average tilt is actually $0.638°$. The area under the probability density function for $1°<θ<∞$ is the probability that $θ>1°$; it is clear that there is a significant probability (14.5%) for this to occur. If realistic values of implanter inaccuracies are assumed instead of the best-case values, this probability rises even higher. This is summarized in Fig. 5.
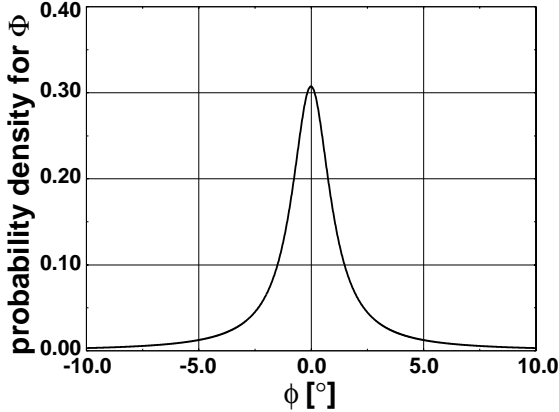

Figure 4(b). Cauchy-like $p_Φ(ϕ)$, from Eqn. 3. The area under the visible part of the curve is $P_Φ(-10° ≤ ϕ ≤ +10°) = 93.4\%$.

Figure 5. Mean value for $Θ$, and $P(θ > 1°)$ for lot #1. For $σ=1°$, $P(θ > 1°)=61\%$. Note that for a Rayleigh-distributed RV, the mean value depends linearly on the $σ$ of the underlying Gaussian RVs.

This is why in Fig. 6 there is a good match between the SIMS measurement and simulation, to a depth of $∼2.0μm$ using a $tilt=1°$. Note that there is still a discrepancy in the tail region between measurement and simulation. This is partly due to a lack of significant statistics (in the Monte Carlo simulation) at that depth. In addition, there are two other possibilities: the neglect of damage due to electronic stopping and secondly, electron gas polarization, which causes implanted ions to experience a non-isotropic and non-uniform force presently ignored in the simulator [3].
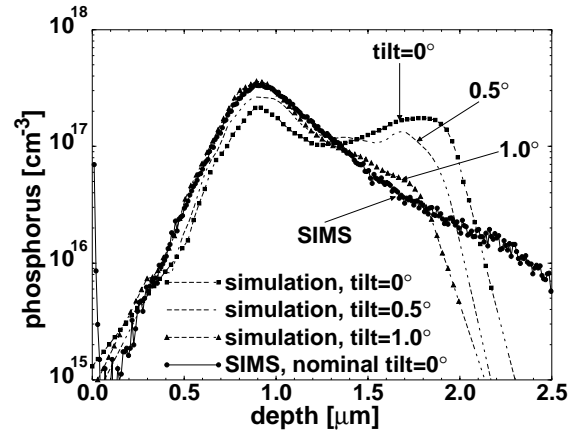

Figure 6. UT-MARLOWE simulations for various tilt-angles, and SIMS data for the $750keV$ phosphorus implant of Fig. 1. Simulations for $tilt=1°$ match SIMS data well (except for the tail-region discrepancy explained in this section).

3   PROCESS DESIGN

Table 2. Statistics for $Θ$ and $Φ$ for the nominally $0°$ tilt implant.

Batch #	tilt ($Θ$)		rotation ($Φ$)	
	average	$P(θ ≥ 1°)$	average	$P(-10° ≤ ϕ ≤ 10°)$
1	$0.638°$	14.5%	$∼0°$	93.4%
2	$0.645°$	15.1%	$∼0°$	93.3%

Integration of the curve in Fig. 4(b) indicates that the rotation angle $ϕ$ is within the range $[-10, +10]$ with a $∼94\%$ probability. Statistical information for $Θ$ and $Φ$ has been summarized in Table 2 and can now be used to design a robust process, using the help of a predictive simulator such as UT-MARLOWE. As shown in Fig. 7(a), for a tilt of $1°$, the simulator predicts no dependence on $ϕ$ in the range $[-10°, +10°]$. The simulator also indicates a strong dependence on $θ$ for $θ < 3°$, but negligible variation for $3° ≤ θ ≤ 5°$ (see Fig. 7(b)). So in order to minimize process-variation, a nominally on-axis implant must actually be centered at $\{θ=4°, ϕ=0°\}$. In cases where $θ=0°$ implants are unavoidable (e.g.: implants into a narrow aperture), $θ=4°$ may be unacceptable. However the methodology proposed here helps quantify the trade-off in process variability in such cases.

In addition to random errors, certain *deterministic* tilt errors occur during ion-implantation, due to beam divergence in a single-wafer machine, or due to process-disk geometry in a multi-wafer machine: the periphery can experience different tilt angles than the center. This results in implant-profile differences and can be seen in SIMS measurements, as demonstrated in Fig. 8. This deterministic error can easily be accounted for in the process design -- given information about the process-disk geometry, the

beam divergence and the wafer size, it is possible to introduce a suitable correction to mean-values of p_Θ and p_Φ. These corrections are in general dependent on the nominal tilt and rotation angles.
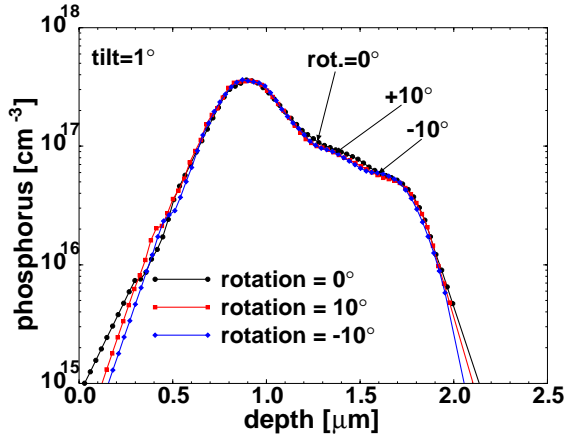

Figure 7(a). UT-MARLOWE simulations for various values of ϕ, with $\theta=1°$. The lack of variability indicates nominal $\phi=0°$ for robustness.
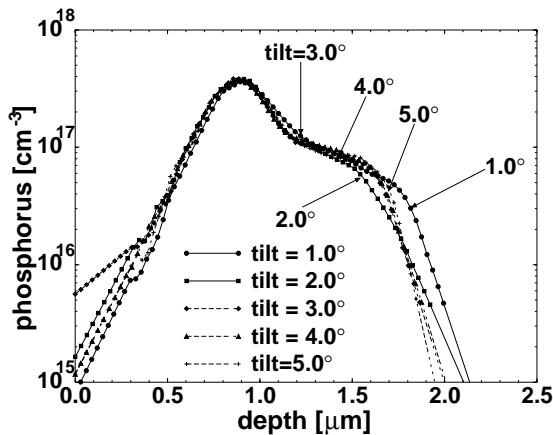

Figure 7(b). UT-MARLOWE simulations for $\theta=1°, 2°, 3°, 4°, and 5°$. The lack of variability for $3°<\theta<5°$ indicates that nominal θ should be $4°$.
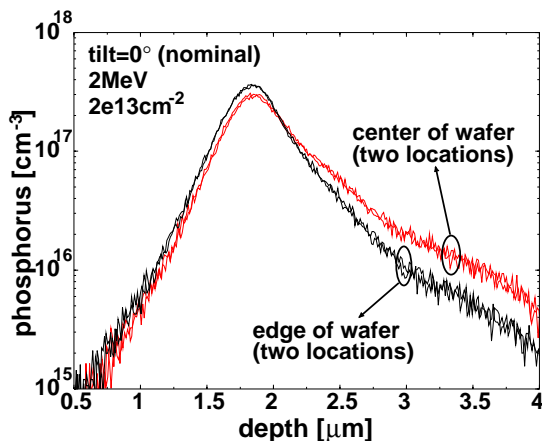

Figure 8. SIMS data for a $2MeV$, on-axis phosphorus implant. Tilt-angle at the edge is quantifyably and *deterministically* larger than at the center.

4   CONCLUSIONS

It has been shown using probability theory that the discrepancy between SIMS measurement and simulated profiles for the example *750keV* phosphorus implant is due to a *~1°* error in the implant angle. This is due to random errors in the crystal cut and implanter alignment, previously unaccounted for. Even with the availability of an accurate implantation simulator, implant errors have to be rigorously accounted for in order to be predictive. Differences in implanted profiles can translate to differences in electrical performance. For instance, if this phosphorus implant formed the n-well region for a PMOS transistor, the well-substrate junction profile and hence the electrical properties of this junction (such as leakage current and breakdown voltage) become strongly dependent on the actual tilt-angle in the implant process. Therefore, for a repeatable process, it is necessary to carefully design the process using the methodology outlined in this work. For the example chosen, the nominally "on-axis" implant has to be centered around $\theta=4°$, $\phi=0°$.

The industry increasingly relies on TCAD methods for reducing technology development costs. This work illustrates the power of introducing statistical methods into traditional TCAD activity. Such a merging of disciplines can benefit not only technology development but also metrology.

ACKNOWLEDGMENTS

REFERENCES

[1] S. Morris, et al, IEEE-IEDM Technical Digest, p. 721-724, 1996.

[2] G. Hobler, et al, IEEE-IEDM Technical Digest, p. 489-492, 1997.

[3] UT-MARLOWE manual, University of Texas at Austin and Los Alamos National Labs.

[4] Data from MEMC Electronic Materials, Inc.

[5] J.N. Kapur & H.K. Kesavan, "Entropy Optimization Principles with Applications," Academic Press, p.62, 1992.

[6] Athanasios Papoulis, "Probability, Random Variables, and Stochastic Processes," McGraw-Hill, 1984.